Dynamics of Atmospheres and Oceans 50 (2010) 78–92

Contents lists available at ScienceDirect

Dynamics of Atmospheres and Oceans

journal homepage: www.elsevier.com/locate/dynatmoce

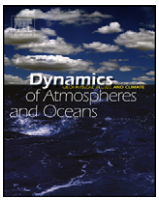

Impact of data assimilation of glider observations in the Ionian Sea (Eastern Mediterranean)

Srdjan Dobricic[a,*], Nadia Pinardi[b,c], Pierre Testor[d], Uwe Send[e]

[a] Centro Euro-Mediterraneo per i Cambiamenti Climatici, Viale Aldo Moro 44, Bologna, Italy
[b] Corso di Scienze Ambientali, Università di Bologna, Italy
[c] Istituto Nazionale di Geofisica e Vulcanologia, Viale Aldo Moro 44, Bologna, Italy
[d] LOCEAN-IPSL, Paris, France
[e] SIO, La Jolla, CA, USA

ARTICLE INFO

Article history:
Received 24 June 2009
Received in revised form 15 January 2010
Accepted 25 January 2010
Available online 4 February 2010

Keywords:
Data assimilation
Glider
Atlantic Ionian Stream

ABSTRACT

Glider observations of temperature, salinity and vertically averaged velocity in the Ionian Sea (Eastern Mediterranean Sea), made in the period October 2004–December 2004, were assimilated into an operational forecasting model together with other in situ and satellite observations. The study area has a high spatial and temporal variability of near surface dynamics, characterized by the entrance of the Atlantic Ionian Stream (AIS) into the Northern Ionian Sea. The impact of glider observations on the estimation of the circulation is studied, and it is found that their assimilation locally improves the prediction of temperature, salinity, velocity and surface elevation fields. However, only the assimilation of temperature and salinity together with the vertically averaged velocity improves the forecast of all observed parameters. It is also found that glider observations rapidly impact the analyses even remotely, and the remote impacts on the analyses remain several months after the presence of the glider. The study emphasizes the importance of assimilating as much as possible all available information from gliders, especially in dynamically complex areas.

1. Introduction

The Mediterranean Forecasting System (MFS) (Pinardi et al., 2003) provides daily analyses of the circulation of the Mediterranean Sea. The analyses are based on the production of background fields

* Corresponding author.
E-mail addresses: srdjan.dobricic@cmcc.it, dobricic@bo.ingv.it (S. Dobricic), n.pinardi@sincem.unibo.it (N. Pinardi).

0377-0265/$ – see front matter © 2010 Elsevier B.V. All rights reserved.
doi:10.1016/j.dynatmoce.2010.01.001

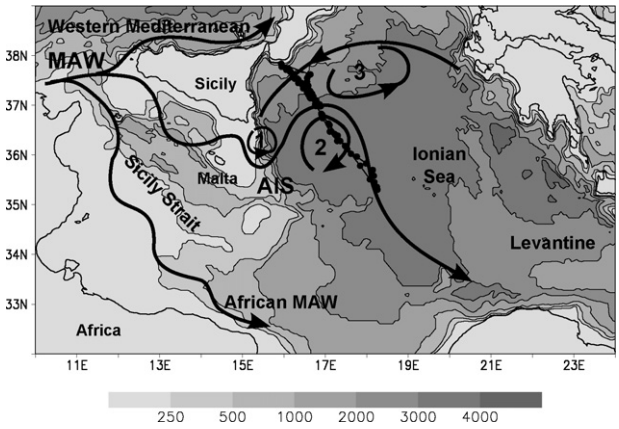

Fig. 1. Bottom topography of the Sicily Strait and the Ionian Sea (m), and path of major surface currents drawn after Pinardi et al. (2006). The dotted line shows the path of the glider in the period October 2004–December 2004. MAW, Modified Atlantic Water; AIS, Atlantic Ionian Stream. Circulation features indexed by numbers are: 1, Ionian Shelf break vortex; 2, Western Ionian anticyclonic gyre; 3, Western Ionian cyclonic gyre.

by a high-resolution general circulation model and the assimilation of in situ and satellite data using a variational assimilation scheme. One of the major challenges of MFS is to assimilate the largest possible number of satellite and in situ observations in real time. The variational multivariate assimilation scheme currently assimilates at the same time satellite Sea Level Anomalies (SLA) and Sea Surface Temperature (SST) and in situ observations of temperature and salinity profiles by eXpendable BathyThermographs (XBT) and Argo floats. The assimilation of observations from additional types of instruments, however, has the potential to provide an improvement in the quality and accuracy of MFS analyses, and MFS started to investigate the importance of gliders that measure temperature, salinity and velocity in the top 200 m of the ocean. The analyses offer the opportunity to study in detail the dynamics of interesting circulation structures, because they produce best estimates of circulation fields based on observations and background states that are dynamically consistent in space and time. In particular, glider measurements, which can be repeated for several months in the same area, could greatly improve estimates of the local circulation. Eventually they may impact analyses even in remote areas.

The glider used here surveyed the central-western Ionian Sea, an area characterized by an intense surface intensified jet stream called the Atlantic Ionian Stream (AIS) (Robinson et al., 1999). The AIS is one of the branches of the Modified Atlantic Water (MAW) stream system that enters the Sicily Strait and occupies the central-northern part of the Strait, near the southern coasts of Sicily (Fig. 1). At the Maltese escarpment, the AIS detaches from the continental shelf and slope region of the Sicily Strait and enters the 3000 m deep Ionian basin. Historical in situ and satellite observations and modeling studies indicate complex circulation patterns of the AIS at the entrance to the Ionian Sea and a high interannual variability (e.g. Malanotte-Rizzoli et al., 1997; Robinson et al., 1999; Lermusiaux and Robinson, 2001; Pinardi et al., 2006). The most detailed investigation of the physical structure and properties of the AIS circulation was obtained with detailed "Conductivity–Temperature–Depth" (CTD) surveys between 1994 and 1996 and by the assimilation of observations into a regional oceanographic model (Robinson et al., 1999; Lermusiaux and Robinson, 2001). Other modeling and observational studies provide somewhat contradictory theoretical explanations for the factors determining the path and the northern extension of the AIS. While studies by Pinardi and Navarra (1993) and Demirov and Pinardi (2002) show that the wind stress curl has an important impact on the seasonal and interannual variability of the circulation in the Northern Ionian Sea, some other studies (e.g. Pierini and Rubino, 2001; Molcard et al., 2002; Napolitano et al., 2003; Sorgente et al., 2003) find that the density gradients mainly influence the path of the AIS.

Additional in situ observations may provide a better understanding of the complex processes that govern the dynamics of the AIS in the Ionian Sea. During its repeated passes in the western Ionian Sea, the glider crossed a meander of the AIS and provided information about the development of the AIS dynamics. The aim of this study is to show the relative impact of glider data assimilation on the quality of the MFS analyses in this area, and to suggest an improved use of the information from glider observations. Section 2 will describe the methodology. It will give an overview of the glider observations, describe the Mediterranean general circulation model and the data assimilation scheme. Section 3 will compare analyses with and without assimilated glider observations to show the impact of the glider observations on the quality of the MFS analyses in the Ionian Sea and the Levantine. Conclusions will be given in Section 4.

2. Data and methods

2.1. Glider observations

Gliders are autonomous underwater vehicles of a small size that can 'fly' underwater along slightly inclined paths by changing their density (Davis et al., 2003). The buoyancy force results in forward velocity (~40 cm/s) as well as vertical motion (~15 cm/s). So gliders move on a sawtooth pattern, gliding downwards when denser than the surrounding water and upwards when buoyant. The high efficiency of the propulsion system enables them to be operated for several months. They can be steered remotely and the measurements can be downloaded during surfacing by a two-way communication system via satellite. When at surface, gliders also take Global Positioning System (GPS) fixes to correct the dead reckoning positions used for navigation. This gives an estimate of the horizontal currents averaged over the glider trajectory between two contact GPS fixes.

In the period 1 October 2004–23 December 2004 a glider from the Webb Research Corporation (Davis et al., 2003) was deployed in the Ionian Sea. The glider made observations of conductivity, temperature, and pressure along a section which spanned ~300 km to the south east of the Italian coast (Fig. 2). It was programmed to dive to 200 m depth and collected 4254 downcasts in about 3 months of operations at a rate of approximately 50 profiles per day; the distance between profiles being approximately 500 m. It had contact with land every eight profiles (~4 h). Classical CTD profiles

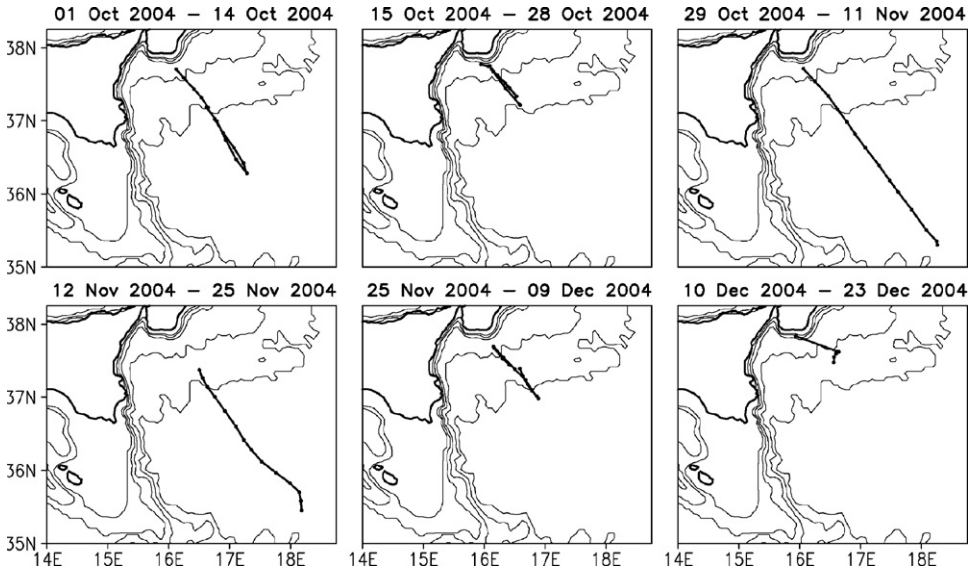

Fig. 2. The path of the glider in the period 1 October 2004–23 December 2004. Dots indicate the daily averaged positions of the glider. The bottom topography is also displayed. Isobaths are 250 m, 500 m, 1000 m, 2000 m and 3000 m.

carried out during the deployment/recovery operations at a few hundred meters from the first/last glider profile allowed the calibration of the conductivity cell in order to match an accuracy of 0.005 PSU in salinity.

2.2. Mediterranean model set-up

The Mediterranean Sea general circulation model set-up (Tonani et al., 2008) is based on the free surface version of the OPA 8.2 code (Roullet and Madec, 2000). Its horizontal resolution is 1/16°, and the domain spans from 18°W to 36°E and 30°N to 46°N. The model covers the whole Mediterranean Sea and includes a part of the Atlantic Ocean. At the boundaries in the Atlantic, temperature and salinity fields are relaxed towards the Levitus climatology (Levitus et al., 1998), and the cross-boundary fluxes are set to zero. The model has 72 levels defined in the vertical. The top level is 3 m thick, and the resolution gradually decreases toward the bottom layers. Horizontal diffusion and viscosity are defined by a bi-Laplacian operator with the constant diffusion coefficient $K_H = 5 \times 10^9\ m^4\ s^1$ and viscosity coefficient $K_M = 3 \times 10^9\ m^4\ s^{-1}$. The vertical diffusion is parameterized in terms of the mixing scheme developed by Pacanowski and Philander (1981), with the addition of enhanced constant vertical value of the mixing coefficient in case of vertical instabilities. The advection of tracers uses a second order accurate upstream scheme (Webb et al., 1998), whilst the momentum advection uses an energy conservative form of the central differencing scheme. Surface fluxes are calculated interactively every 6 h (Castellari et al., 1998) by bulk formulations using atmospheric fields of air temperature, humidity, winds and cloud cover from the operational analyses of the European Centre for Medium-range Weather Forecasts (ECMWF). Surface heat fluxes in the model are corrected by a term proportional to the difference between the temperature at the top model layer and objective analyses (Buongiorno Nardelli et al., 2002) of the satellite SST. The coefficient of relaxation applied in the surface heat fluxes correction is $40\ W\ m^{-2}\ K^{-1}$. A detailed description of the model set-up is given in Tonani et al. (2008). The model simulation initial condition is set to correspond to January 1 2002 using the temperature and salinity MEDATLAS climatology (The MEDAR Group, 2002).

2.3. Data assimilation scheme

The data assimilation scheme is the three-dimensional variational scheme called OceanVar and developed for oceanographic models (Dobricic and Pinardi, 2008). The scheme models the background error covariances through the control space transformation by a successive application of linear operators. The vertical part of temperature and salinity background error covariances is represented by most significant Empirical Orthogonal Functions (EOFs) of their long-term variability. The control space contains weights that in the first linear operator multiply each EOF in order to produce vertical profiles of temperature and salinity corrections. Then the second operator models horizontal covariances, assumed to be isotropic Gaussian functions of horizontal distance, by successive applications of recursive filters and by taking into account the presence of coastlines. Once the three-dimensional corrections are estimated for temperature and salinity fields, the third operator estimates the corresponding sea level corrections. It is a barotropic oceanographic model that finds the steady state sea level distribution corresponding to the constant forcing by the vertically averaged buoyancy force calculated from corrections in temperature and salinity. The last two operators estimate baroclinic velocity components by applying the geostrophic relationship in the presence of the coastlines. A detailed mathematical description of linear operators is given in Dobricic and Pinardi (2008).

The horizontal background error covariances have the correlation radius of 15 km. This value is estimated empirically from the evaluation of the horizontal correlation of misfits between background fields and SLA observations in the period 2001–2004. The analyses are not very sensitive to small variations of this parameter. As the Rossby radius of deformation in the Mediterranean is about 10–15 km (e.g. Robinson et al., 1987) the corresponding typical length scale of eddies is 50–100 km (Stammer, 1997; Eden, 2007) and the used correlation scale is smaller than the average eddy size. Multivariate EOFs used to represent the background error correlations in the vertical direction are estimated from sea level, temperature, salinity and barotropic stream function covariances. However, in OceanVar only temperature-salinity covariances from EOFs are used in practice, and covariances with the sea

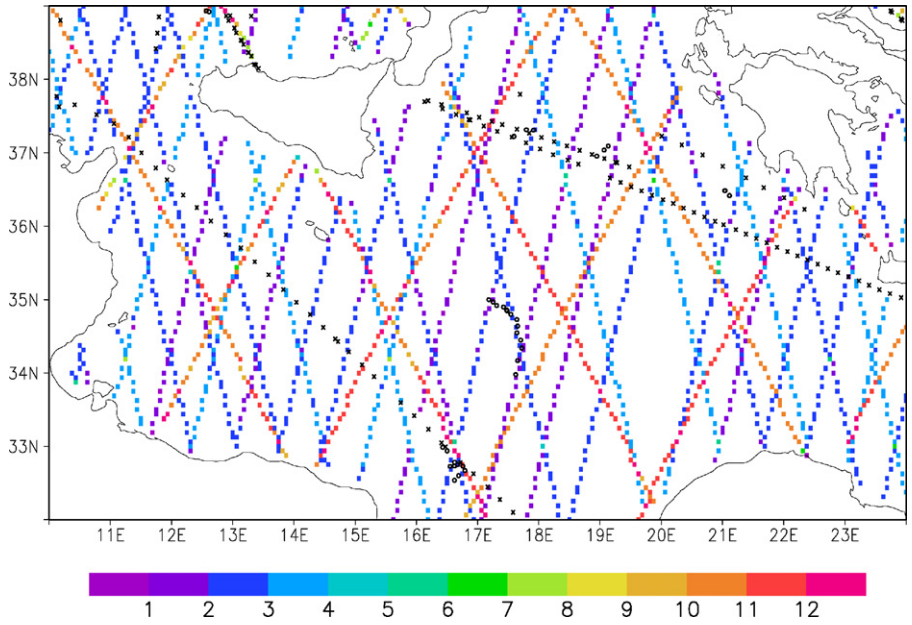

Fig. 3. Observations assimilated in all experiments during the period under study (October 2004–March 2005). Colored squares show the number of SLA observations in each model grid point. Each satellite measured SLA at least twice in the same grid point. Crosses indicate points where temperature profiles were measured by the XBTs and circles indicate positions of observations of temperature and salinity profiles by Argo floats. (For interpretation of the references to color in this figure legend, the reader is referred to the web version of the article.)

level and the barotropic component of velocity are estimated by the application of a barotropic model in each iteration of the minimizer. The EOFs are calculated with covariances between four parameters because they are also used in an optimal interpolation scheme in which it is not possible to dynamically model covariances with sea level and barotropic components of velocity (Dobricic et al., 2005). The Mediterranean Sea is divided into 13 regions with different physical properties, and 20 EOFs are calculated in each region and for each season from the variability around the mean of a model run spanning the time period 1993–2000. All the details of the methodology to estimate vertical EOFs are found in Dobricic et al. (2005, 2007).

In order to calculate misfits temperature, salinity and sea level background fields are linearly interpolated to the positions of observations. The observations are assimilated only in areas deeper than 150 m, because it is assumed that more shallow areas are dominated by coastal processes and there observations are inappropriate for the deep ocean analyses. The background SLA estimates are obtained by subtracting the Mean Dynamic Topography (MDT) from the background sea level field. A new observational operator is constructed in OceanVar in order to assimilate observations of the vertically averaged velocity. First it horizontally interpolates daily averaged background velocities on the daily averaged position of the glider and then vertically averages interpolated values. Like velocity observations background velocity is averaged over the 1 day long period spanning the length of each short-term simulation in order to remove the inertial oscillations.

The analyses are produced starting from 1 June 2004 with a daily assimilation cycle. The MDT is estimated successively by correcting the estimate by Rio et al. (2007) with unbiased estimates from in situ observations used in the operational assimilation system. This methodology to correct MDT is described in Dobricic (2005). Fig. 3 shows the observational coverage of SLA and in situ temperature and salinity observations in the Ionian Sea and the Sicily Strait. We can see that SLA observations cover the whole area with a high frequency. On the other hand, in situ observations are distributed unevenly and have a limited spatial and temporal coverage. Clearly, the introduction of glider observations in

the area where the AIS enters the Ionian Sea could improve locally the quality of ocean state estimates and also provide an information about accuracy of the estimates based only on the assimilation of SLA observations, because during this period there are no other in situ observations in the area.

3. Assimilation of glider observations

Given the assumed horizontal error correlation scale of 15 km, glider observations spaced ∼500 m would not be independent. Therefore the raw observations were averaged within a 12 h long time window, giving rise to observations spaced approximately 12 km. This spacing is represented by approximately two model grid points at 1/16 degrees model resolution. This further justifies the averaging of observations, because any corrections at spatial scales shorter than two grid points cannot be represented by the model finite difference scheme and would be removed as noise during the model integration. The observations are also averaged in the vertical direction by producing a single averaged observation at each model level. It is important to notice that the vertical averaging does not produce completely independent observations, because the vertical dimension in the control space is reduced to 20 EOFs. These vertical dependencies, however, did not seem to have any impact on the rate of the convergence of the minimizer (not shown).

Hereafter we refer to 'control' experiment as the experiment with the assimilation run without glider data, but with the assimilation of all satellite SLA and Argo and XBT in situ observations. This section will compare control experiment to experiment which in addition assimilated glider observations, so-called glider experiment. Analyses from the control and glider experiments will be called control and glider analyses, respectively. Furthermore, the rms of misfits will be calculated between observations and short-term simulations starting from the analyses. Simulations that start from control analyses will be called control simulations. In addition there will be three glider experiments. In the first experiment analyses assimilate only temperature and salinity, in the second only velocity, and in the third temperature and salinity together with velocity.

Fig. 4 shows a Hovmoller diagram of the daily averaged glider observations for temperature. In autumn 2004, the vertical stratification changed from a shallow thermocline in October (around 30 m deep) to a weaker and deeper thermocline in November, and to an almost vertically homogeneous water column in December. The control analyses were capable to reproduce the high vertical stratification in October, the deepening of the mixed layer in November and the enhanced vertical mixing in December, but did not depict some of the mesoscale features that were observed by the glider, and the thermocline was diffuse. For example, the glider observations show a large deepening of isotherms, probably corresponding to anticyclonic motion, on October 10, October 30 and November 8, whereas the control analyses show only a weak signal. Due to the differences at mesoscales, the correlation of temperature in the top 100 m between observations and control analysis was 0.60. On the other hand, the glider assimilation analyses show that these mesoscale features were introduced by the assimilation of glider observations, and the correlation of temperature between the observations and glider analyses was 0.81.

Daily averaged observations of salinity are shown in Fig. 5. The observed minima of salinity, corresponding to the core of MAW, show the position of the AIS in agreement with previous observations (e.g. Lermusiaux and Robinson, 2001). In October the salinity minimum is located at the depth of ∼40 m. Its position becomes deeper in November, and reaches ∼60 m on December 1. Furthermore, in November the salinity minimum extends from the ocean surface to the depth of ∼50 m, indicating enhanced vertical mixing. Fig. 5 shows also that the control analyses are in general capable to depict the major path of the AIS but they do not capture some small scale structures at the depth of ∼50 m during the periods October 5–15 and October 28 to November 10. This inability to depict mesoscale features gives the correlation of salinity in the top 100 m between observations and control analyses of 0.39. The assimilation of glider observations corrects the salinity field (Fig. 5) in the proper direction and produces a marked minimum of the salinity at ∼50 m. The improved representation of mesoscale features increases the correlation of salinity between observations and glider analyses to 0.81. The assimilation also increases the mean salinity along the path of the glider in accordance with the in situ observations.

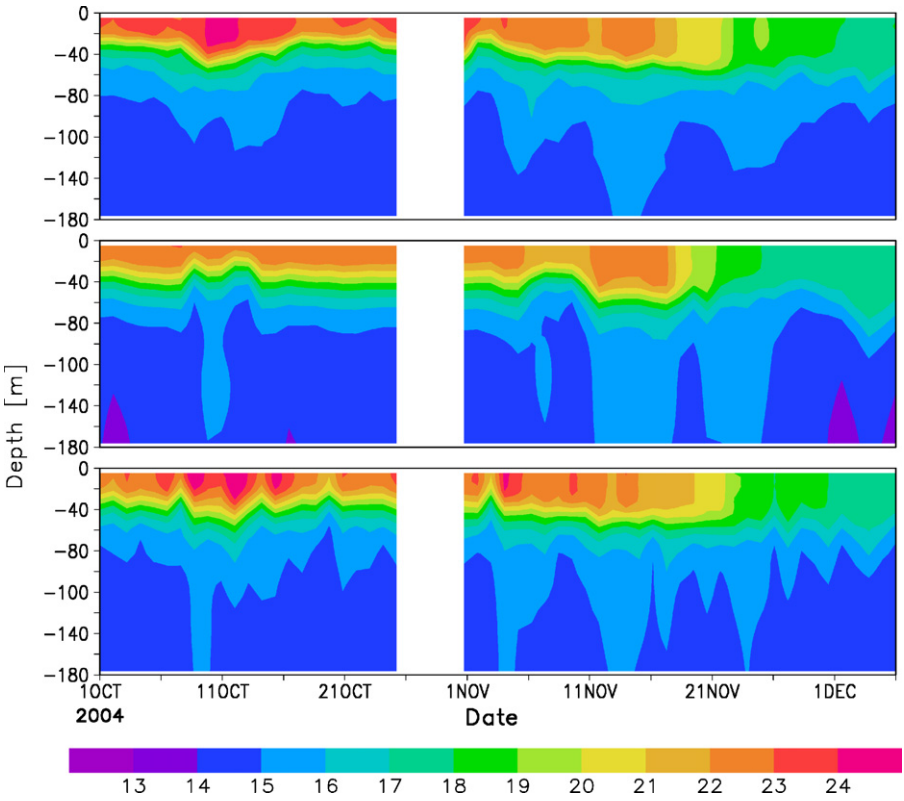

Fig. 4. Daily averaged vertical temperature profiles (°C) along the path of the glider for the period October–December 2004. Upper panel: glider observations, averaged daily; Middle panel: control daily analyses. Lower panel glider assimilation analyses. Between October 25 and October 30 the glider was in the area shallower than 150 m, and the observations were automatically discarded by OceanVar as "coastal observations".

We may conclude that along the path of the glider the horizontal position of the anticyclonic meander of the AIS, characterized by the low salinity, was generally well depicted by the control analyses in periods October 6–14, November 4–18, and November 21–28. However, the glider observed more variability at smaller scales. It is important to notice that in each of periods October 6–14 and November 4–18 the glider changed the direction at the borders of the AIS and crossed twice its core. On the other hand control analyses show a very smooth area of low salinity, which also has the minimum close to the surface instead at the depth of 50 m. We may explain the agreement in the horizontal position of the anticyclonic meander of the AIS by the fact that control analyses assimilated a large number of SLA observations (see Fig. 3). They constrained the near surface flow to depict the position of the AIS in a general accordance with in situ observations. The absence of in situ observations in control analyses, however, introduced larger uncertainties in the estimates of vertical profiles. The vertical temperature and salinity gradients appeared more diffusive than observed, the mean salinity was lower than observed, and the minimum of the salinity was close to the surface. The insertion of in situ observations by the glider clearly improved the estimate of vertical structures and removed the salinity bias.

The impact of the assimilation of glider observations is further emphasized in Table 1 which compares the rms of misfits between the control experiment, the experiment with the assimilation of only temperature and salinity observations by the glider, the experiment with the assimilation of only velocity observations by the glider and the experiment with the assimilation of temperature and salinity together with velocity observations. A single rms of each parameter is calculated during the

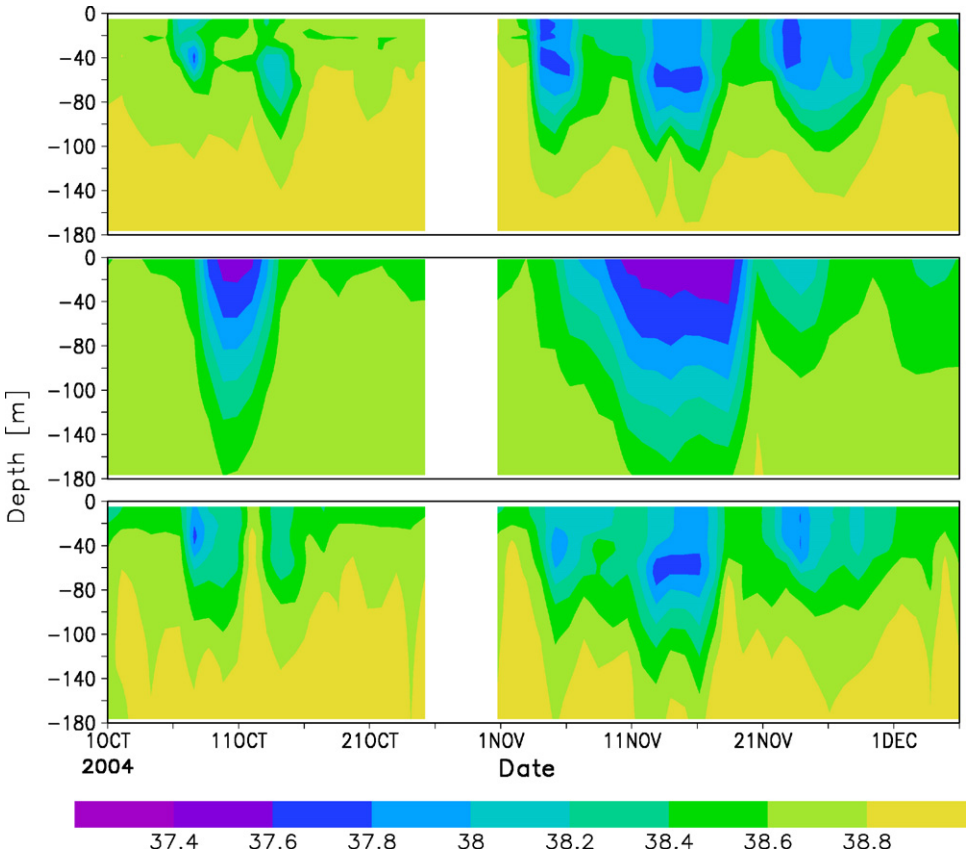

Fig. 5. Same as Fig. 3, but for salinity.

Table 1
The rms of misfits for temperature observations in the top 50 m ($\overline{\mathrm{rms}(T)}^{0-50\ \mathrm{m}}$) and from 50 m to 200 m depth ($\overline{\mathrm{rms}(T)}^{50-200\ \mathrm{m}}$) in °C, for salinity observations in the top 50 m ($\overline{\mathrm{rms}(S)}^{0-50\ \mathrm{m}}$ c) and from 50 m to 200 m depth ($\overline{\mathrm{rms}(S)}^{50-200\ \mathrm{m}}$), rms for the zonal component ($\mathrm{rms}(\bar{u}^{0-200\ \mathrm{m}})$), for the meridional component ($\mathrm{rms}(\bar{v}^{0-200\ \mathrm{m}})$), for the magnitude of the vertically averaged velocity ($\mathrm{rms}(|\bar{v}^{0-200\ \mathrm{m}}|)$) in ms^{-1} and rms for SLA in cm. When glider observations are assimilated the rms estimates the accuracy of the simulation in the next day. The control experiment is marked by "Control", the experiment assimilating temperature and salinity profiles only by "*T*, *S*", and the experiment assimilating temperature and salinity profiles and the vertically averaged velocity by "*T*, *S*, *v*". The lowest rms for all three experiments is underlined for each parameter.

	Control	*T*, *S*	*v*	*T*, *S*, *v*
$\overline{\mathrm{rms}(T)}^{0-50\,\mathrm{m}}$	1.47	0.90	2.14	<u>0.86</u>
$\overline{\mathrm{rms}(T)}^{50-200\ \mathrm{m}}$	0.46	<u>0.31</u>	0.51	<u>0.31</u>
$\overline{\mathrm{rms}(S)}^{0-50\ \mathrm{m}}$	0.39	0.22	0.48	<u>0.21</u>
$\overline{\mathrm{rms}(S)}^{50-200\ \mathrm{m}}$	0.28	0.13	0.30	<u>0.11</u>
$\mathrm{rms}(\bar{u}^{0-200\ \mathrm{m}})$	0.101	0.121	<u>0.080</u>	0.091
$\mathrm{rms}(\bar{v}^{0-200\ \mathrm{m}})$	0.087	0.089	0.082	<u>0.059</u>
$\mathrm{rms}(\lvert\bar{v}^{0-200\ \mathrm{m}}\rvert)$	0.096	0.118	0.090	<u>0.083</u>
rms(SLA)	4.06	4.10	<u>3.79</u>	<u>3.79</u>

period of glider observations (October 1 to December 23). The rms of misfits represents an independent estimate of the quality of the estimates because it computes the difference between simulations starting from the analysis and observations before the observations are assimilated. Thus, it estimates the accuracy of the analyses by comparing short-term simulations to independent observations. If we assume that the most of the errors present in short-term simulations are due to the errors in the initial conditions, we may assume the rms of misfits provides an independent estimate for the accuracy of the analyses. Temperature and salinity misfits are calculated only with respect to glider observations, because there are no other in situ observations close to the glider. In addition to the rms of temperature and salinity misfits the table shows the results for the rms of misfits for the u and v components and the magnitude of the velocity averaged in the top 200 m of the water column with respect to glider observations. When glider observations are assimilated the rms estimates the accuracy of 1 day long simulations. Furthermore, Table 1 shows the rms of SLA misfits in the vicinity of the glider. It is calculated from satellite SLA observations appearing in a circle with the radius of 110 km around each glider observation during 5 days after the glider observation. The 5 days long period is the minimum repeat time for the SLA observations. It should be noticed that simulations are still 1 day long and that there are new glider observations inside each circle in the following days. However, there is no replication of SLA misfits in the calculation of the rms. The chosen maximum spatial and temporal distance between SLA and glider observations provides 334 SLA misfits and consequently ensures the robustness of the statistics. The variations in the distance from 55 km to 220 km and in the temporal window from 2 to 7 days gave qualitatively similar results (not shown). The area of 110 km is significantly larger than 15 km of the horizontal covariance radius. Therefore, by choosing 110 km we expect that the information from glider observations is rapidly spread in a much larger area than the correction. As it will be shown later in this section the information from the glider observations indeed seems to spread very rapidly.

The table shows that the assimilation of only temperature and salinity observations clearly improves the short-term prediction of temperature and salinity (by 30–50%). However, it also worsens the prediction of velocity and SLA. The reason for this result could be that in the horizontal direction OceanVar uses an isotropic correlation function which may be inappropriate in an area with strong dynamics where both SLA and velocity fields have high temporal and spatial variations. When only the vertically averaged velocity is assimilated the rms of velocity misfits improves. It is interesting that also the rms of SLA misfits improves (by 8%). However the rms of temperature misfits near surface becomes significantly worse then in the control experiment (by 45%) as well as the rms of salinity misfits near the surface (by 23%). We may explain this result by the fact that the errors in the gradient of the surface elevation are efficiently reduced by assimilating in situ observations of velocity. On the other hand, in the absence of in situ temperature and salinity observations the inaccurate vertical structure of mass corrections balancing velocity corrections leads to less accurate temperature and salinity fields. As it could be expected, the assimilation of velocity, together with temperature and salinity profiles, improves the rms of velocity misfits (by 30%). However, just like the assimilation of velocity only it also significantly reduces the rms of SLA field (by 8%). Furthermore, it systematically reduces the rms of temperature and salinity misfits (up to 15%). In fact the experiment which assimilates the velocity in addition to temperature and salinity predicts most accurately all parameters. While eventually it could be expected for SLA misfits, the reduction of temperature and salinity misfits in the experiment which assimilates glider temperature, salinity and velocity compared to the experiment which assimilates temperature and salinity only may be somewhat surprising. First, one can exclude that errors in vertical EOFs impact the result, because it is reasonable to assume that with in situ observations accurate vertical profiles of background error covariances are not essential to obtain the accurate vertical structure of the corrections. There are enough observations of temperature and salinity in the vertical profile that define very accurately the vertical structure of the corrections, and it can be assumed that 20 EOFs are sufficient to fit closely almost any vertical structure of error covariances determined by misfits along the profile. In fact, when temperature and salinity observations were assimilated after the correction vertical profiles of temperature and salinity matched very closely those observed by the glider (not shown). Second, the MDT errors can also be excluded, because in the experiment that assimilated only glider velocity the in situ velocity observations appeared to be consistent with SLA observations resulting in the reduction of the rms of SLA misfits. Eventually, a reason for improvements

due to the assimilation of velocity in addition to temperature and salinity could be that the corrected velocity field advects in a more realistic way the temperature and salinity, therefore, produces a lower misfit at subsequent times. The experiment which assimilates velocity only indicates that, however, this is not the case, as it gives significantly worse rms of misfits for both temperature and salinity in comparison to all other experiments. Thus, it seems that the assimilation of temperature and salinity gives accurate corrections in the vertical structure of the temperature and salinity fields, while due to the mass balance constraints the assimilation of velocity further improves horizontal gradients of temperature and salinity corrections. In summary, the main advantage of assimilating velocity in addition to temperature and salinity seems to be to improve the horizontal, and therefore, the full three-dimensional structure of the corrections. Clearly, this form of the positive impact may be very important in dynamically complex areas like the AIS.

It is interesting to evaluate how much the improvements obtained by the assimilation of glider observations impact the general structure of the surface flow in the Northern Ionian Sea. Fig. 6 shows the sea level at the end of the period by glider observations in the glider assimilation and control

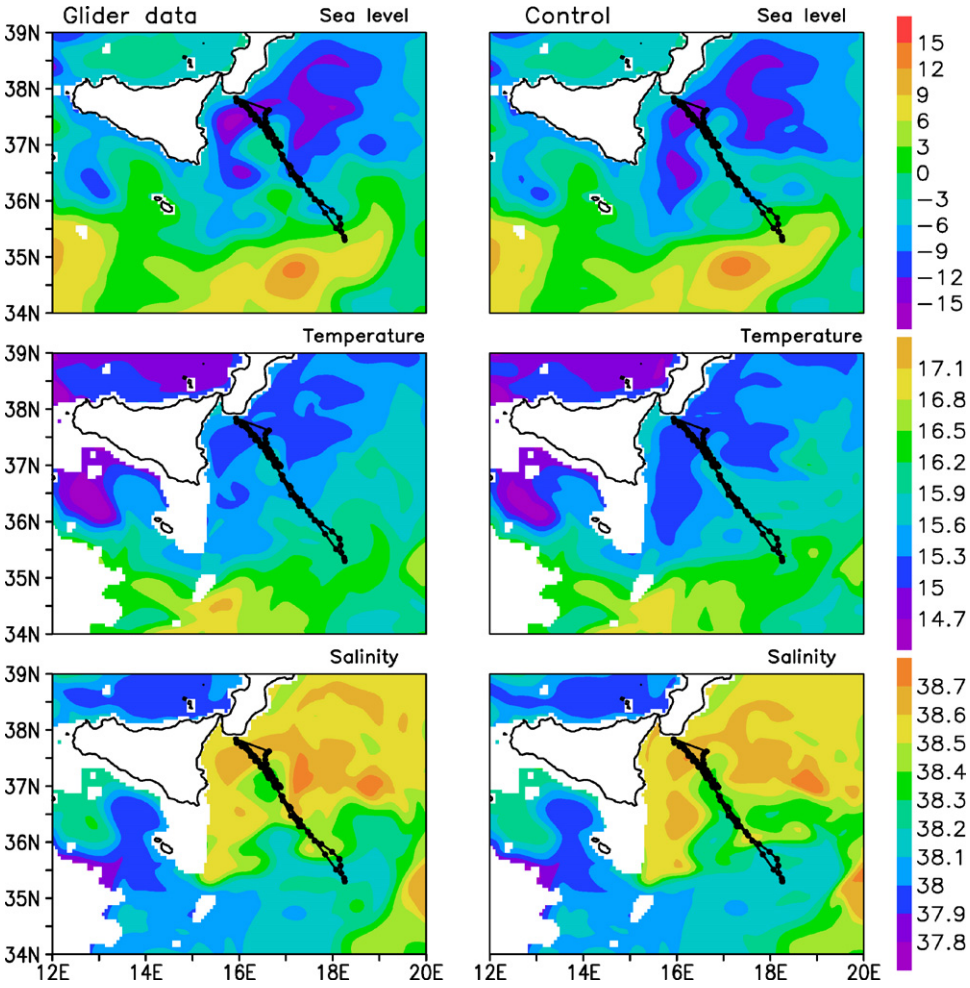

Fig. 6. Comparing daily averaged fields between glider assimilation (left) and control (right) analyses on 23 December 2004. Top panels show surface elevation (cm), middle panels mean temperature (°C) in the top 200 m and bottom panels mean salinity (PSU) in top 200 m.

experiments. Its general structure is very similar in both experiments even along the glider path. In both experiments the AIS, marked by the high gradient of the surface elevation, enters the Ionian Sea at 35°N flowing eastwards. At 16°E it turns northward, forms an anticyclonic meander up to 38°N, turns back southwards to 37°N, and then flows eastwards towards the Levantine. All eddies in two experiments are positioned at the same places. However, they slightly differ in shape and intensity. These differences give a smaller rms of SLA misfits in the experiment which assimilated glider data. When temperature and salinity averaged over the top 200 m are compared, both experiments show a similar penetration of warm and fresh MAW into the Northern Ionian Sea forming the Western Ionian anticyclonic Gyre. However, the experiment with glider data shows higher temperatures and lower salinity of the Ionian waters that flow southwards along the Sicilian coast. The high general similarity in the sea level field was observed throughout the period of glider observations (not shown). It can be concluded that, although the assimilation of glider observations improved the estimate of the smallest scales, most of the features of the sea level field in the control experiment were in a good general agreement with the observations by the glider.

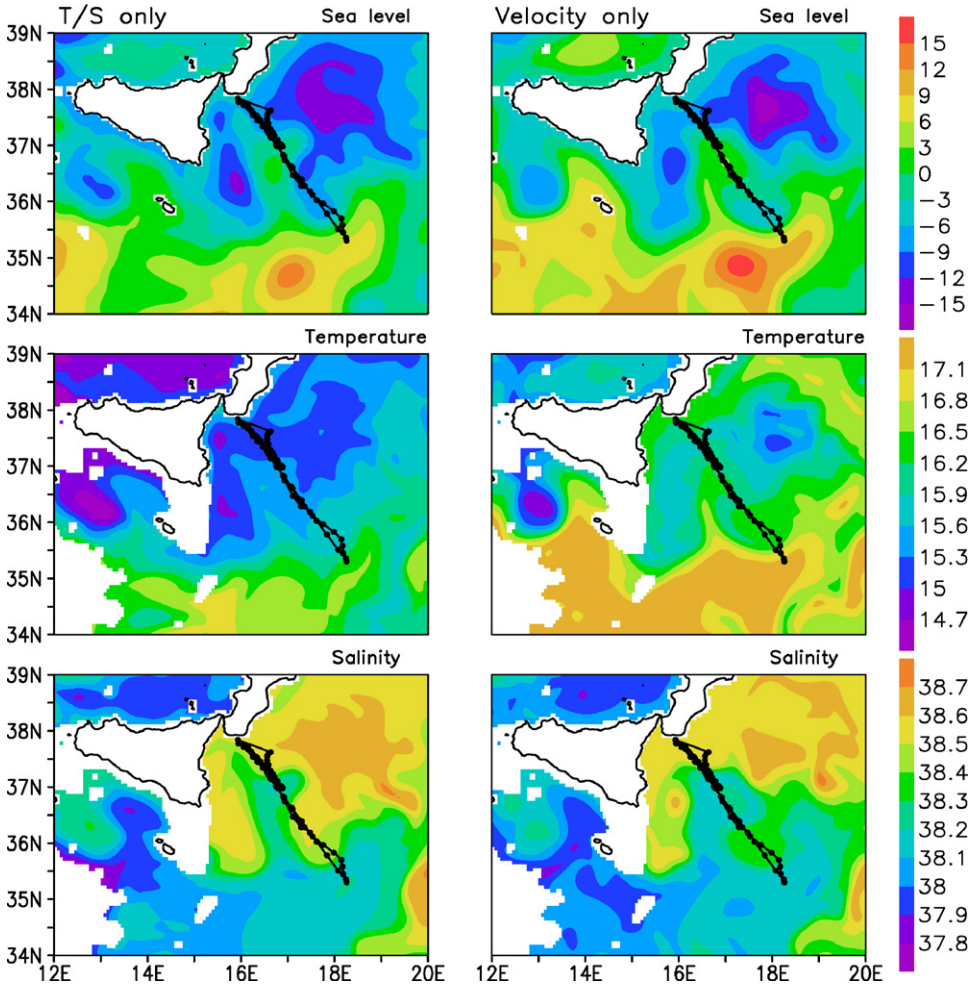

Fig. 7. Same as Fig. 6, but for the analysis that assimilated only temperature and salinity profiles (left), and only vertically averaged velocity (right).

It is also interesting to see how the assimilation of only temperature and salinity, and only velocity impacted the general structure of the near surface flow at the end of the assimilation of glider data. Fig. 7 shows that in the case of the assimilation of only temperature and salinity the anticyclonic meander extends further to the north until it reaches the coast and cuts in two the area occupied by Ionian waters. A larger quantity of MAW is advected northwards, and Ionian waters advected southwards along the Sicilian coast have even lower temperature than in the control experiment. Fig. 7 further shows that in the case of the assimilation of only velocity the anticyclonic meander extends similarly like in the control experiment, but temperature is much higher along the path of the glider. Furthermore, temperature is increased south of the AIS, and the near surface circulation is modified even in the Sicily Strait. It is clear from the rms of misfits shown in Table 1 that near surface analyses shown in Fig. 7 are less accurate than those given by the experiment assimilating all glider data (Fig. 6).

Fig. 8 shows differences between analyses by the glider experiment and the control experiment during and after the presence of glider observations. Initially, during October and November, the differences are located along the path of the glider. However, at the end of December, 3 months after the first glider observations, the differences are spread in an area extending about 1000 km to the east. They further grow and reach the maximum at the end of February, about 2 months after the last glider observation. During March the differences are slowly attenuated. The differences spread rapidly, because OceanVar finds the global minimum of the cost function over the whole Mediterranean. This means that changes of the cost function due to the presence of additional observations in a small area may rapidly impact the solution in remote places. In fact, it can be seen in Fig. 8 that there are

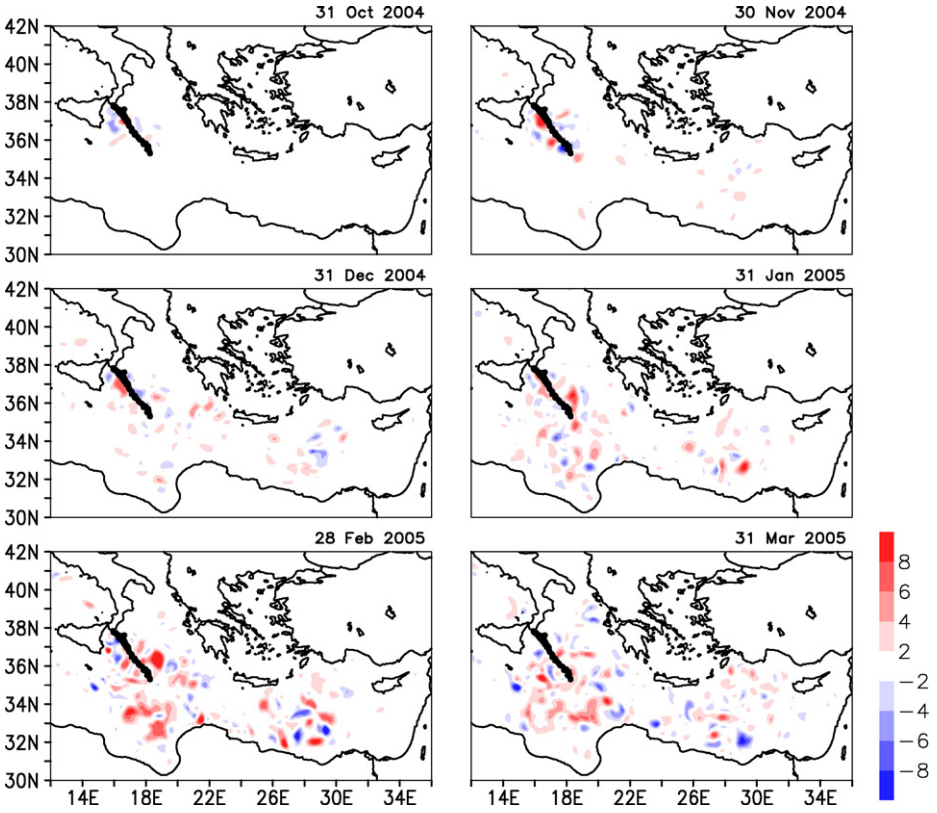

Fig. 8. Daily averaged sea level differences between glider and control experiments (cm). The differences are shown at the end of each of 6 months following the introduction of glider observations.

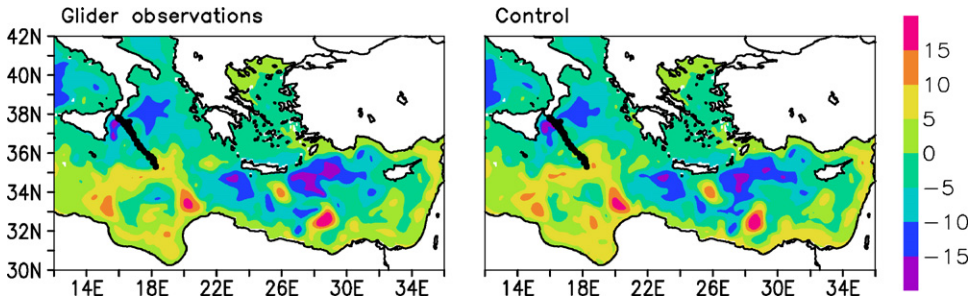

Fig. 9. Daily averaged sea level field (cm) on 28 February 2005 corresponding to the day with the largest differences shown in Fig. 8. The left panel shows the glider analysis, and the right panel shows the control experiment.

small remote differences already at the end of November. Furthermore, at the end of December the differences in the Levantine are as large as those close to the glider position. Fig. 9 shows the sea level field in the Levantine in control and glider analyses at the end of February when the remote differences have the largest intensity. It can be seen that at 30°E the coastal current detaches from the coast in a form of a free jet. In this area it could be expected that remote differences can become large due to the strong dynamics. Even after the presence of the glider the differences may grow by the fast dynamical processes, because different background states give different minima of the cost function. However, the same SLA observations are continuously assimilated in both experiments. Slowly they attenuate the differences between the two sets of analyses, and at the end of March they are reduced in comparison to those at the end of February. Fig. 9 further shows that even at the end of February when the differences were the largest, both analyses show a very similar position of eddies. They mainly differ in the shape and the intensity. The fact that the sea level analyses from the two experiments are very similar is emphasized by the weekly rms of SLA misfits in the area from 14°E to 30°E (Fig. 10). Even in February–March the difference between the rms of SLA misfits in two experiments is small, although the experiment assimilating glider observations has a slightly higher accuracy. It is important to notice that the rms of SLA misfits is very close to the estimated error of satellite SLA observations of about 3 cm (Menard et al., 2003). Therefore, it is difficult to improve it significantly in remote areas by the assimilation of additional observations.

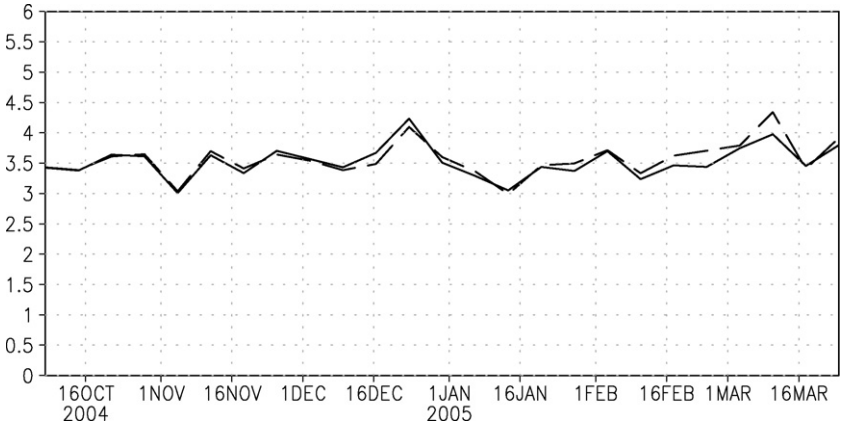

Fig. 10. The weekly rms of SLA misfits (cm) calculated over the area from 14°E to 30°E (see Fig. 8). The full line shows the glider experiment, and the dashed line the control experiment.

4. Conclusions

The study has shown that the assimilation of temperature, salinity and velocity observations from a glider monitoring experiment in the Ionian Sea locally improved the Mediterranean Forecasting System (MFS) analyses. It reduced the fresh bias in the salinity field and represented more accurately the Modified Atlantic Water (MAW) subsurface maxima along the Atlantic Ionian Stream (AIS) path. Either the assimilation of only temperature and salinity profiles or of only vertically averaged velocity had a negative effect on the accuracy of some analyzed parameters. On the other hand, the assimilation of temperature and salinity profiles, together with the velocity observations increased the accuracy of all analyzed fields. This result emphasizes the importance of assimilating the information on the vertically averaged velocity estimated by the glider, especially in dynamically complex areas. It should be noticed that the velocity is not the directly observed variable, but it is derived from the observed drift of the glider. Therefore, it would be more advantageous to directly assimilate the drift by forming an observational operator in the form of a Lagrangian trajectory. A similar observational operator is already operative in OceanVar for the assimilation of the drift data from Argo floats (Taillandier et al., in press), and in the future could be applied to gliders, too.

The study of the differences between the control analyses and the analyses that assimilated glider observations showed that the information from the glider initially is located in the area close to the glider observations. However, the impact of glider observations spreads rapidly to remote areas and differences between glider and control analyses growth even a few months after the last observation by the glider. The remote impact of glider observations in remote areas appears to be slightly positive. The fast spreading of the information by the glider observations to remote areas may be explained by the properties of the OceanVar data assimilation scheme that globally adjusts all fields during the minimization of the cost function. Once the background states are modified remotely the differences from the control analyses may persists for months and even growth. However, on the long-term the assimilation of a large number of SLA observations in both glider and control analyses attenuates the differences.

The study shows that the glider observations locally improved the quality of the basin scale analyses. They also had a visible impact on the surface circulation in remote areas that was persistent several months after the last glider observation. Several new deep ocean gliders are being deployed in the Mediterranean. They are capable to measure temperature, salinity and velocity down to 1000 m and we may expect that they will improve the quality of the basin scale analyses.

Acknowledgements

We would like to thank two unknown reviewers for their comments and suggestions which significantly improved the presentation of our findings. This work was partially funded by EU projects MFSTEP (Mediterranean Forecasting System: Towards Environmental Predictions, Contract Number: EVK3-CT-2002-00075) and MERSEA (Marine Environment and Security for the European Area, Contract Number: SIP3-CT-2003-502885). Special thanks to Giuseppe Zappalà of the Istituto Talassografico of Messina who helped with the logistics of the glider experiment.

References

Buongiorno Nardelli, B., Larnicol, G., D'Acunzo, E., Santoleri, R., Marullo, S., Le Traon, P.Y., 2002. Near real time SLA and SST products during 2-years of MFS pilot project: processing, analysis of the variability and of the coupled patterns. Ann. Geophys. 21, 103–121.

Castellari, S, Pinardi, N., Leaman, K.D., 1998. A model study of air–sea interactions in the Mediterranean Sea. J. Mar. Syst. 18, 89–114.

Davis, R.E., Eriksen, C.E., Jones, C.P., 2003. Autonomous buoyancy-driven underwater gliders. In: Griffiths, G. (Ed.), Technology and Applications of Autonomous Underwater Vehicles. Taylor and Francis, pp. 37–58.

Demirov, E., Pinardi, N., 2002. Simulation of the Mediterranean Sea circulation from 1979 to 1993. Part I: the interannual variability. J. Mar. Syst. 33-34:, 23–50.

Dobricic, S., Pinardi, N., Adani, M., Bonazzi, A., Fratianni, C., Tonani, M., 2005. Mediterranean Forecasting System: an improved assimilation scheme for sea-level anomaly and its validation. Q. J. Roy. Meteor. Soc. 131, 3627–3642.

Dobricic, S., 2005. New mean dynamic topography of the Mediterranean calculated from assimilation system diagnostics. Geophys. Res. Lett. 32, L11606, doi:10.1029/2005GL022518.

Dobricic, S., Pinardi, N., Adani, M., Tonani, M., Fratianni, C., Bonazzi, A., Fernandez, V., 2007. Daily oceanographic analyses by Mediterranean Forecasting System at the basin scale. Ocean Sci. 3, 149–157.
Dobricic, S., Pinardi, N., 2008. An oceanographic three-dimensional variational data assimilation scheme. Ocean Modell. 22, 89–105.
Eden, C., 2007. Eddy length scales in the North Atlantic Ocean. J. Geophys. Res. 112, doi:10.1029/2006JC003901.
Lermusiaux, P.F.J., Robinson, A.R., 2001. Features of dominant mesoscale variability, circulation patterns and dynamics in the Strait of Sicily. Deep Sea Res. 48, 1953–1997.
Levitus, S., Boyer, T.P., Conkright, M.E., O'Brien, T., Antonov, J., Stephens, C., Stathoplos, L., Johnson, D., Gelfeld, R., 1998. NOAA Atlas NESDIS 18 World Ocean Database 1998. U.S. Gov. Printing Office, Washington, DC, 346 pp. (+ set of Cd-roms).
Malanotte-Rizzoli, P., Manca, B.B., Ribera D'Alcala, M., Theocharis, A., Bergamasco, A., Bregant, D., Budillon, G., Civitarese, G., Georgopoulos, D., Michelato, A., Sansone, E., Scarazzato, P., Souvermezoglou, E., 1997. A synthesis of the Ionian Sea hydrography, circulation and water mass pathways during POEM-Phase I. Prog. Oceanogr. 39, 153–204.
The MEDAR Group, 2002. MEDAR/MEDATLAS 1998–2001 Mediterranean and Black Sea Database of Temperature, Salinity and Bio-chemical Parameters and Climatological Atlas (4 CDRoms). Internet server www.ifremer.fr/sismer/program/medarIFREMER/TMSI/IDM/SISMER, Ed., Centre de Brest.
Menard, Y., Fu, L.-L., Escudier, P., Parisot, F., Perbos, J., Vincent, P., Desai, S., Haines, B., Kunstmann, G., 2003. The Jason-1 mission. Mar. Geod. 26, 131–146.
Molcard, A., Gervasio, L., Griffa, A., Gasparini, G.P., Mortier, L., Özgökmen, T.M., 2002. Numerical investigation of the Sicily Channel dynamics: density currents and water mass advection. J. Mar. Syst. 36, 219–238.
Napolitano, E., Sannino, G., Artale, V., Marullo, S., 2003. Modeling the baroclinic circulation in the area of the Sicily Channel: the role of stratification and energy diagnostics. J. Geophys. Res. 108, 3230, doi:10.1029/2002JC001502.
Pacanowski, R.C., Philander, S.G.H., 1981. Parameterization of vertical mixing in numerical models of tropical oceans. J. Phys. Oceanogr. 11, 1443–1451.
Pierini, S., Rubino, A., 2001. Modeling the oceanic circulation in the area of the Strait of Sicily: the remotely forced dynamics. J. Phys. Oceanogr. 31, 1397–1412.
Pinardi, N., Navarra, A., 1993. Baroclinic wind adjustment processes in the Mediterranean Sea. Deep Sea Res. 40, 1299–1326.
Pinardi, N., Allen, I., Demirov, E., De Mey, P., Korres, G., Lascaratos, A., Le Traon, P.-Y., Maillard, C., Manzella, G., Tziavos, C., 2003. The Mediterranean ocean forecasting system: first phase of implementation (1998–2001). Ann. Geophys. 21, 3–20.
Pinardi, N., Arneri, E., Crise, A., Ravaioli, M., Zavatarelli, M., 2006. The physical, sedimentary and ecological structure and variability of shelf areas in the Mediterranean Sea. In: Robinson, A.R., Brink, K. (Eds.), The Sea, vol. 14. Harvard University Press, Cambridge, USA, pp. 1243–1330.
Rio, M.E., Poulain, P.-M., Pasqual, A., Mauri, E., Larnicol, G., Santoleri, L., 2007. A mean dynamic topography of the Mediterranean Sea computed from the altimetric data and in situ measurements. J. Mar. Syst. 65, 484–508.
Robinson, A.R., Hecht, A., Pinardi, N., Bishop, J., Leslie, W.G., Rosentroub, Z., Mariano, A.J., Brenner, S., 1987. Small synoptic/mesoscale eddies and energetic variability of the eastern Levantine basin. Nature 327, 131–134.
Robinson, A.R., Sellschopp, J., Warn-Varnas, A., Leslie, W.G., Lozano, C.J., Haley, P.J., Anderson, L.A., Lermusiaux, P.F.J., 1999. The Atlantic Ionian Stream. J. Mar. Syst. 20, 129–156.
Roullet, G., Madec, G., 2000. Salt conservation, free surface and varying volume: a new formulation for ocean GCMs. J. Geophys. Res. 105, 23927–23942.
Sorgente, R., Drago, A.F., Ribotti, A., 2003. Seasonal variability in the Central Mediterranean Sea circulation. Ann. Geophys. 21, 299–322.
Stammer, D., 1997. Global characteristics of ocean variability estimated from regional TOPEX/POSEIDON altimeter measurements. J. Phys. Oceanogr. 27, 1743–1769.
Taillandier, V., Dobricic, S., Testor, P., Pinardi, N., Griffa, A., Mortier, L., Gasparini, G.P., in press, Integration of Argo trajectories in the Mediterranean Forecasting System and impact on the regional analysis of the western Mediterranean circulation, J. Geophys. Res., doi:10.1029/2008JC005251.
Tonani, M., Pinardi, N., Dobricic, S., Adani, M., Marzocchi, F., 2008. A high resolution free surface general circulation model of the Mediterranean Sea. Ocean Sci. 4, 1–14.
Webb, D.J., deCuevas, B.A., Richmond, C.S., 1998. Improved advection schemes for ocean models. J. Atmos. Ocean. Technol. 15, 1171–1187.